

Reliable experimental data as a key factor for design of mechanical structures

Josip Brnic^{1a}, Sanjin Krscanski^{1b}, Marino Brcic^{*1}, Lin Geng^{2c}, Jitai Niu^{2d} and Biao Ding^{3e}

¹Department of Engineering Mechanics, University of Rijeka, Faculty of Engineering, Vukovarska 58, Croatia

²School of Material Science and Engineering, Harbin Institute of Technology, 92 West Dazhi St., Harbin 150001, PR China

³College of Material Science and Engineering, Shanghai University, Shanghai 200072, PR China

(Received March 9, 2019, Revised June 26, 2019, Accepted July 5, 2019)

Abstract. The experimentally determined mechanical behavior of the material under the prescribed service conditions is the basis of advanced engineering optimum design. To allow experimental data on the behavior of the material considered, uniaxial stress tests were made. The aforementioned tests have enabled the determination of mechanical properties of material at different temperatures, then, the material's resistance to creep at various temperatures and stress levels, and finally, insight into the uniaxial high cyclic fatigue of the material under different applied stresses for prescribed stress ratio. Based on fatigue tests, using modified staircase method, fatigue limit was determined. All these data contributes the reliability of the use of material in mechanical structures. Data representing mechanical properties are shown in the form of engineering stress-strain diagrams; creep behavior is displayed in the form of creep curves while fatigue of the material is presented in the form of S-N (maximum applied stress versus number of the cycles to failure) curve. Material under consideration was 18CrNi8 (1.5920) steel. Ultimate tensile strength and yield strength at room temperature and at temperature of 600°C: [$\sigma_{m,20/600} = (613/156)$ MPa; $\sigma_{0.2,20/600} = (458/141)$ MPa], as well as endurance (fatigue) limit at room temperature and stress ratio of $R = -1$: ($\sigma_{f,20,R=-1} = 285.1$ MPa).

Keywords: Steel 18CrNi8; mechanical properties; creep behavior and creep modeling; fatigue and fatigue limit

1. Introduction

The choice of the material of structure should be consistent with the purpose of the structure, its operating conditions and its lifetime. In accordance with this, material selection is one of the most difficult task for any designer, since besides mentioned requests related to service conditions, material availability and cost of the material should be considered. It is known that material properties depend on its chemical composition, processing path and resulting microstructure, Bramfit (1997). However, properties have to correspond to the working (service) conditions of the structure because they determine its mechanical behavior. The choice of materials is also related to the material shaping process, Ashby (2011). The design of the structures is usually carried out under the assumption that there is no failure in the material as well as in the design process, and assuming that the failure will not occur during the production, exploitation, control (inspection) or maintenance of the structure. All mentioned can be met but very rare. Engineering practice usually shows quite the opposite. In this sense, in engineering practice two general

groups of failures can be mentioned, and that pre-existing failures and failures that can occur during structure life including its design process, service life, testing, control (inspection) and maintenance. To the pre-existing failures can be counted, for example, pre-existing defects in material, pre-existing cracks or that occur from imperfections. Engineering element can be manufactured as smooth, notched or cracked. The following mechanical failures can appear in the engineering elements (Stephens *et al.* 2001, Collins 1993, Brooks and Choudhury 2002): misuse, design error, improper material, improper maintenance, inadequate control, assembly error, manufacturing defects, excess deformation (elastic, yielding, onset of plasticity), buckling, wear, corrosion, creep - excess deformation, fatigue – repeated loading (corrosion fatigue, creep-fatigue), impact, the transition of temperature effect, etc. A particular failure or more of them together, can lead to great damage, dysfunctionality of the structure, fracture, or even human casualties. Engineering discipline, such as analysis of failures in engineering structures, has the purpose to find out why and how a particular structure has experienced a fracture. Since a particular structural failure has its cause of origin as well as the form of its manifestation, it is possible to determine why and how considered structural element has failed, Brnic (2018) and Brnic (2013). Some of common observed failure modes in engineering practice, mentioned above, are recognized as possible causes of failures that can lead to the damage or fracture of the element. Based on this, an answer why an element has failed can be obtained. From the other hand, in a similar way, based on the form of manifestation of the failure, an answer how structural element has failed

*Corresponding author, Professor
E-mail: brcic@riteh.hr

^a D. Sc.

^b D. Sc.

^c D. Sc.

^d D. Sc.

^e D. Sc.

can be obtained. In this paper, several possible failure modes were considered and that: excess deformation including elastic and plastic parts as well as yielding, then creep and fatigue of the material. Although 18CrNi8 steel is well-known in engineering practice and has been studied by numerous researchers, this investigation provides to the practitioners readily available data about mechanical behavior of this material at different environmental conditions. Firstly, as far as extension is concerned, it is expressed through engineering stress-strain diagrams. Furthermore, with regard to creep resistance, it can be distinguished by the creep curves. Creep as the phenomenon that arises in (metallic) material as inelastic strain usually is defined as time-dependent material behavior at which deformation continues to increase is kept constant, Solecki and Conant (2003). Briefly, creep means growth of strains under stress uniform in time, Drozdov (1996), i.e., it means a tendency of a material to its progressively deform over time under a constant stress (load). Creep is more significant at higher load levels and higher temperature levels. It is possible that particular structural element will experience creep due to its own weight at high temperature. In engineering practice permitted creep strains are the most up to a level of 2%. Creep at metallic material is usually appreciable at temperature above 0.4 of its melting temperature, Raghavan (2004). Finally, it is known that repeated load significantly reduce static strength of the material. In accordance with this, fatigue (endurance) limit need to be determined as a relevant measure in designing dynamically stressed components. Below are some papers that deal with issues related to the considered steel 18CrNi8. In Xu and Yu (2015) the problem of fractured injector nozzles made of 18CrNi8 steel is considered. On the basis of visual inspection and fractographic investigation the position of the crack origin is determined. Machinability characteristics of alloy and stainless steel bars, including 18CrNi8 steel, have been considered and compared to each other, Jana *et al.* (2001). Investigation of the correlation between hardenability and microstructure has been carried out on the low carbon steel 1.5920 after the pack carburization process, Hosseini *et al.* (2013). The problem of getting micro holes on metal alloys, including 18CrNi8 steel, by electrochemical machining (ECM) process, was been considered in Kong *et al.* (2017). The study dealing with the carburizing process of low carbon steel (18CrNi8) is presented in Hosseini (2012). Further, in Kabira and Bulpett (2007) are presented comparative results obtained by testing engine components under extreme operating conditions with those obtained from laboratory tests. Experimental investigations related to the fatigue properties of 18CrNi8 steel with different heat treatment processes have been carried out. In order to gain insight into the mechanical behavior of some structures made of particular materials, as well as into possible comparison their properties with the material studied here or other materials, it is recommended to consider the following published papers. In the paper written by Zhang *et al.* (2019), behavior of bridge girders under localized fire exposure conditions is considered. In

Table 1 Chemical composition: 18CrNi8 steel

Material: 18CrNi8 steel (Alloyed carbon steel)							
Designation							
Steel name (type, grade, quality) / i.e., letter mark of steel in accordance with the norm (country code): (EN, DIN and other norms)				Steel number (Mat. No; W. Nr; Mat. Code) / i.e., numerical designation of steel			
[EN] / [DIN]: [10084 (1998)] / [17210 (1986)]:				1.5920			
18CrNi8 GB 18Cr2Ni2							
Chemical composition Mass (%)							
C	Si	Mn	P	S	Cr	Ni	Mo
0.19	0.24	0.48	0.01	0.01	1.9	1.8	0.091
Cu	Al	W	Co	Rest			
0.156	0.013	0.024	0.027	95.059			

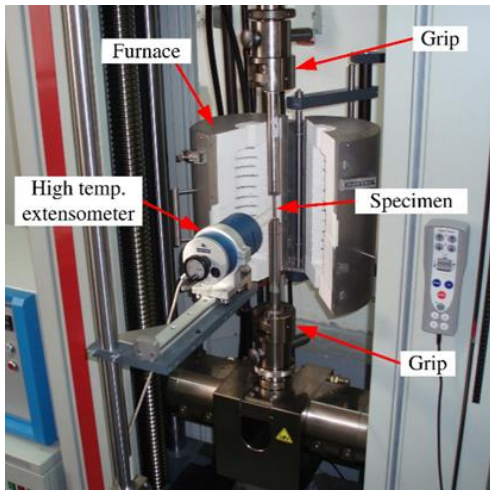
addition, testing and analysis of the results of uniaxial behavior of low alloy steel (42CrMo8) is presented in Brnic *et al.* (2016). In addition, experimental and numerical research of the column under compressive loads made of steel SHS are shown in Shahraki *et al.* (2018).

2. Data related to used material, type of testing, equipment, specimens, testing procedures and standards

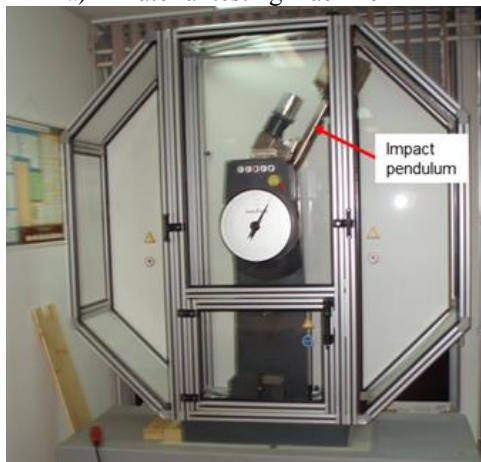
Material - under consideration in this investigation is annealed 18CrNi8 steel, shaped as round bar of 20 mm diameter. Supplier gave no other information regarding the material. It is known as alloyed carbon steel or, sometimes, as Cr-Ni-alloyed case hardening steel. Its chemical composition is shown in Table 1. As possible engineering applications of this material can be mentioned engineering components with large cross-sections requiring high toughness and core strength as well as other structural members. These components may be gears, crankshafts, heavy-duty shafts and other elements in mechanical engineering, aircraft industry, truck constructions, etc. The case - hardening steel 18CrNi8 can be used for highly stressed components of the automotive industry and general in mechanical engineering. Parts of injection nozzles in modern diesel injection systems usually is made of this material.

The Equipment that was used for testing the mechanical properties of the material at different temperatures as well as for the creep testing of the material is Zwick / Roell material testing machine capacity of 400kN, Fig. 1a. In the field of high temperatures, for strain determination, high temperature extensometer (Mytech) and furnace (max 900°C) were used. Further, Charpy impact machine (300J) was used in determination of impact energy, Fig 1b, while Servopulser (± 50 kN) was used in fatigue testing, Fig 1c.

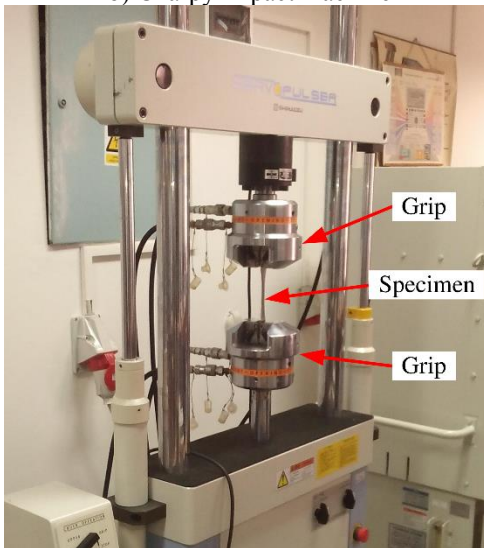
Two different testing modes were performed. One of them is uniaxial testing that relates to the determination of



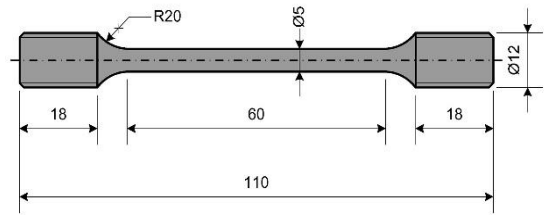
a) Material testing machine



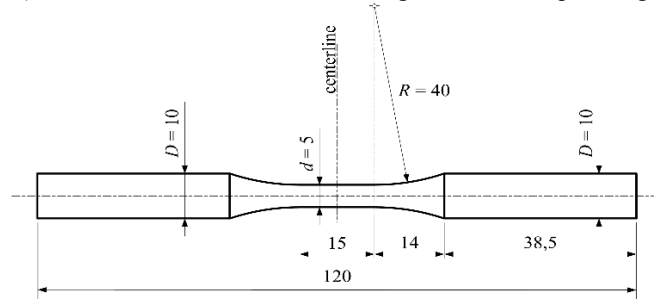
b) Charpy impact machine



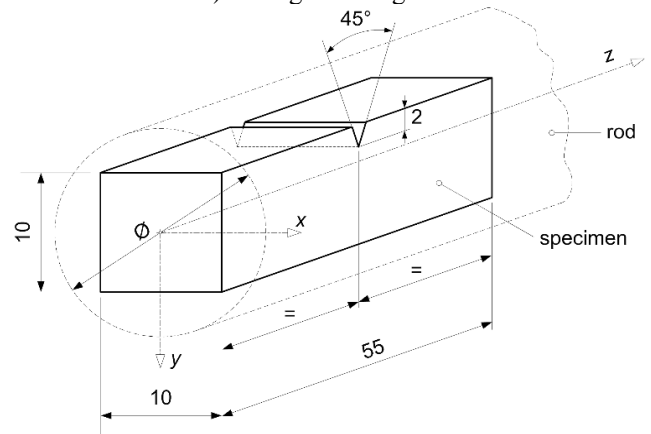
c) Dynamic testing machine
Fig. 1 Experimental equipment



a) Determination of stress-strain diagrams and creep testing



b) Fatigue testing



c) Charpy impact energy testing

Fig. 2 Specimens used in testing procedures

as well as in creep behavior determination are defined by the standard ASTM E8 / E8M - 16a, Fig.2a. Shape and geometry of the specimens used in fatigue testing can be found in ISO 12107:2012, Fig 2b. A specimen of dimensions 55 x 10 x 10 mm was used in Charpy V-notch impact energy testing, Fig. 2c. Specimens were shaped by turning work of the same rod.

3. Results of experimental research and discussion

3.1 Material mechanical behavior and mechanical properties versus temperature

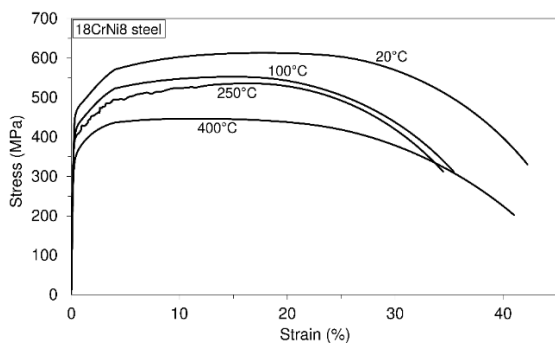
Engineering stress-strain diagrams that indicate the behavior of material at different temperatures, and on which it is possible to determine the mechanical properties of the material, are shown in Fig.3. For each applied temperature, several specimens were tested. Differences in the resulting curves (engineering diagrams) related to the same applied test temperature can be considered negligible. For this reason, Fig. 3 shows the curves relating to the first test at

mechanical properties, material creep behavior, and fatigue of the material. Other one relates to the determination of fracture impact energy.

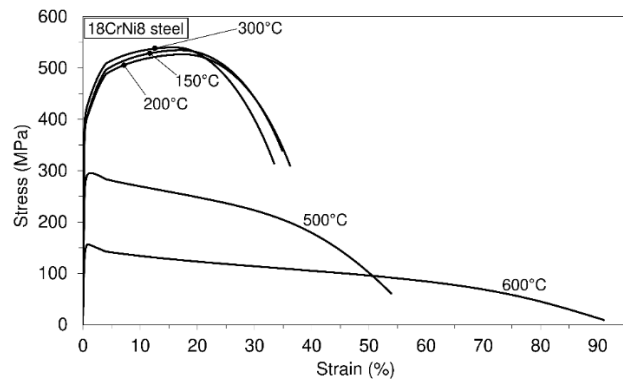
Shape and geometry of Specimens used in the tests to obtain mechanical properties at room and high temperatures

Table 2 Data on mechanical properties: 18CrNi8 steel

Temp. T (°C)	Ultimate tensile strength (σ_m), yield strength ($\sigma_{0.2}$) and modulus of elasticity (E)				Reduction factor, $f = F_{i,T}/F_{i,20}$; $F_i = \sigma_m, \sigma_{0.2}, E$			Total strain (ε_t) and reduction in area (ψ): data relating to the specimen	
	σ_m (MPa)	$\sigma_{0.2}$ (MPa)	Ratio $\sigma_{0.2}/\sigma_m$	E (GPa)	$\sigma_{m,T}$ $/\sigma_{m,20}$	$\sigma_{0.2,T}$ $/\sigma_{0.2,20}$	$E_{,T}$ $/E_{,20}$	ε_t (%)	ψ (%)
20	613	458	0.747	215	1	1	1	42	76
100	552	412	0.746	207	0.9	0.9	0.963	38	77
150	535	383	0.716	203	0.873	0.836	0.944	35	71
200	527	392	0.744	197	0.86	0.856	0.916	36	75
250	536	400	0.746	190	0.874	0.873	0.884	34	74
300	540	410	0.759	181	0.881	0.895	0.842	34	72
400	447	349	0.781	176	0.729	0.762	0.819	41	76
500	295	276	0.936	139	0.481	0.603	0.646	54	89
600	156	141	0.904	81	0.254	0.308	0.377	91	96



(a) Temperature: 20°C, 100°C, 250°C, 400°C



(b) Temperature: 150°C, 200°C, 300°C, 500°C, 600°C

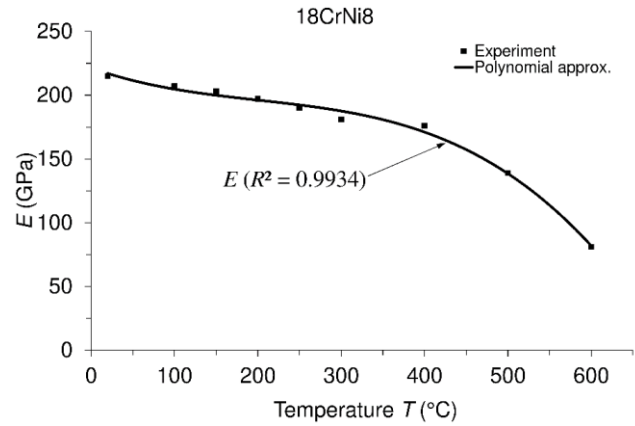
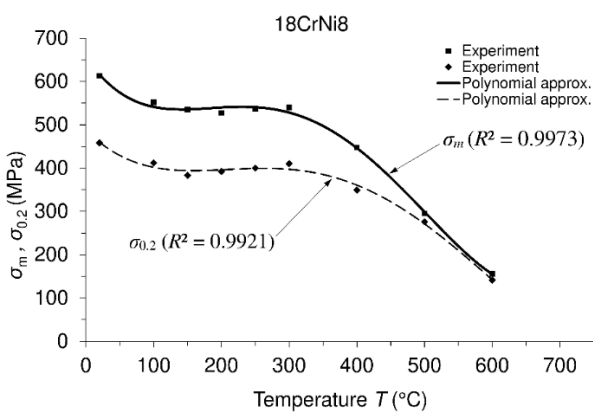
Fig. 3 Engineering stress-strain diagram at different temperature (first test for each applied temperature), 18CrNi8 steel

each applied temperature. The mentioned experimentally determined mechanical properties are of remarkable significance because they indicate the possibility of using the material. Numerical data relating to the mechanical properties, obtained based on the mentioned stress-strain diagrams are presented in Table 2. Modulus of elasticity has been tested by regression method available in Zwick-testXpert software using speed of testing of 10MPa/s at room temperature and 5MPa/s at elevated temperatures. Each of the considered properties has the highest value at room temperature. After the room temperature the value of ultimate tensile strength and the value of yield strength decreases, and then, the new relative increase in value occurs at a temperature of 300°C for each of mentioned properties. Temperature dependences of mechanical properties are displayed in Fig. 4. Each experimentally obtained result is displayed by a special character (■) or (♦). Polynomial approximations of the experimentally obtained results are shown using solid or dashed line. As a measure of accordance between experimental results and polynomials is used the coefficient (R^2). It serves, as statistics giving information about how fit a model is, Draper and Smith (1998). Based on Fig. 3 and Table 2, a

local maximum of strengths (at 300°C) is a consequence of dynamic strain aging, which is a hardening phenomenon.

3.2 Creep tests and creep modeling

Knowing the behavior of a material under the influence of high temperatures is extremely important for the applications of the material in such situations. High temperatures can be manifested in predictable working processes or in undesirable failures, fire, hazards or the like. The behavior of the creep of material can be analyzed based on real creep tests or simulated creep tests. Simulated creep tests can denote modeled tests of actual creep processes or may indicate predictable creep tests. Predictable creep tests may relate to situations that are similar to those for existing processes (but may be different in the level of temperature or in the level of the applied stress) of the same or similar materials. However, in this study short-time creep behavior was considered which is consistent with the possible application of the material. Namely, due to its application, it is possible to temporarily heat of the material, a fire or other shorten hazard situation. Experimentally obtained creep curves as well as data defining creep processes are shown in



a) Ultimate tensile strength (σ_m) and yield strength ($\sigma_{0.2}$)

b) Modulus of elasticity (E)

$$\sigma_m(T) = 2.68682 \cdot 10^{-8} T^4 - 3.68361 \cdot 10^{-5} T^3 + 1.48648 \cdot 10^{-2} T^2 - 2.2974 \cdot T + 656.424$$

$$\sigma_{0.2}(T) = 1.20706 \cdot 10^{-8} T^4 - 1.94786 \cdot 10^{-5} T^3 + 9.01277 \cdot 10^{-3} T^2 - 1.57911 \cdot T + 487.783$$

$$E(T) = -1.33916 \cdot 10^{-6} T^3 + 8.05813 \cdot 10^{-4} T^2 + 2.33882 \cdot 10^{-1} T + 221.367$$

Fig. 4 Mechanical properties (σ_m , $\sigma_{0.2}$ and E) versus temperature (T) - experimental results and polynomial approximations, 18CrNi8 steel

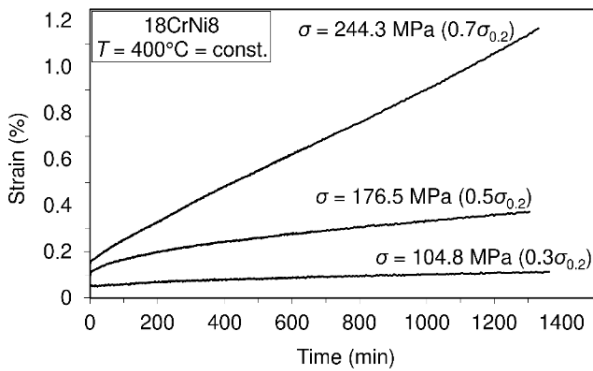


Fig. 5 Creep behavior of 18CrNi8 steel at $T = 400^\circ\text{C}$

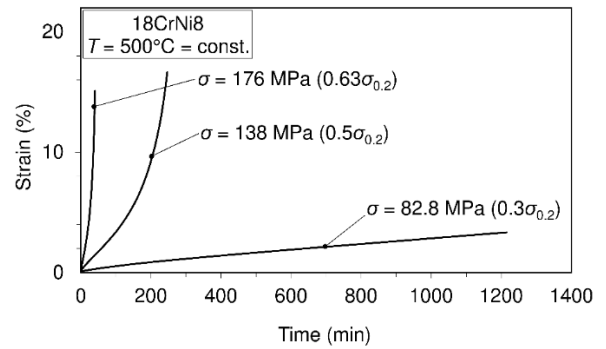


Fig. 6 Creep behavior of 18CrNi8 steel at $T = 500^\circ\text{C}$

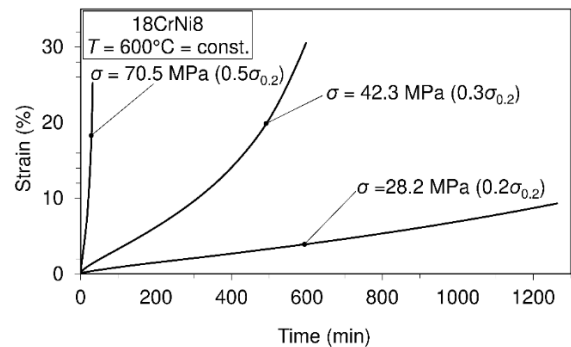


Fig. 7 Creep behavior of 18CrNi8 steel at $T = 600^\circ\text{C}$

Figs. 5-7. Creep processes are carried out at certain constant temperatures. At a certain constant temperature the creep process is performed for a certain constant stress level. As previously mentioned, testing the creep process can take more time and requires expensive equipment, so sometimes the simulation / prediction of creep process can be done based on already known similar process. Modeling / simulation of a creep process can be carried out using rheological models or using some of known analytical formulas that can be found in Brnic (2018), Findley *et al.* (1989), Solecki and Conant (2003) as well as in Boresi *et al.* (1993). Since in engineering practice it is allowed to occur only a few percent of the creep strains, here will be shown creep modeling only for creep processes that are the constituent parts of the first and / or second creep stage. Namely, the third creep stage surely contains great creep strains and tends to the fracture of the considered engineering element. Mentioned creep stages are: first creep stage (I - primary creep / transient creep), second creep stage (II - secondary creep / steady- state creep), third creep stage (III - tertiary creep / accelerating creep). In addition to

the large number of formulas used to model / simulate the creep process, the two rheological models most commonly used in modeling are the Burgers model and the Standard Linear Solid (SLS) model, Brnic (2018).

Since both the recommended rheological models as well as the recommended formula give similar images of modeled creep curves, only modeled creep curves obtained using formula will be displayed to avoid overlapping the images. The formula (equation) in question, which serves to model the creep curve, is of the form (Brnic *et al.* 2013)

Table 3 Data related to creep modeling

Material	18CrNi8 (1.5920)		
Combined Time – Temperature – Stress Dependent Model: $\epsilon(t) = \epsilon(\sigma, T, t)$ ↓ Applied Model → $\epsilon(t) = D^{-T} \sigma^p t^r$ [Equation (1)]			
Time (min) = 1200 Creep processes were carried out at temperatures and stresses listed below			
Constant temperature $T(^{\circ}C)$	400		500
Applied constant stress level $\sigma(Pa)$	$104.8 \cdot 10^6$	$176.5 \cdot 10^6$	$82.8 \cdot 10^6$
$\sigma = x \cdot \sigma_{0.2}$	$x = 0.3$	$x = 0.5$	$x = 0.3$
Parameters	Parameters (D, p, r) valid for:		
	$x = 0.3 - 0.5$		$x \leq 0.3$
$D, p, r \rightarrow$ determined by $\epsilon(t) =$	D	1.11821095708496	2.40680283366159
Strain determination: $\epsilon(t) = D^{-T} \sigma^p t^r$	p	2.18844952804439	23.8598957274256
$T(^{\circ}C); \sigma(Pa); t(min)$	r	0.291161060148216	0.749320497372521

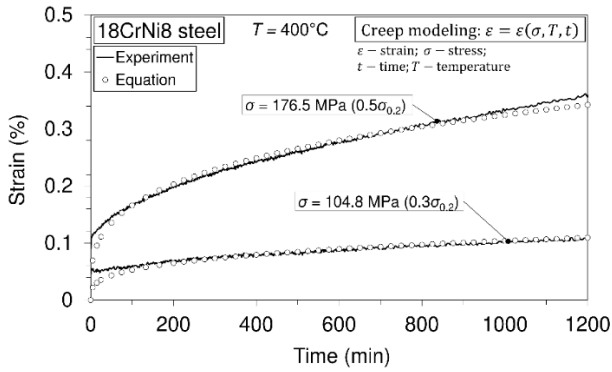


Fig. 8 Creep modeled curves at temperature of 400°C

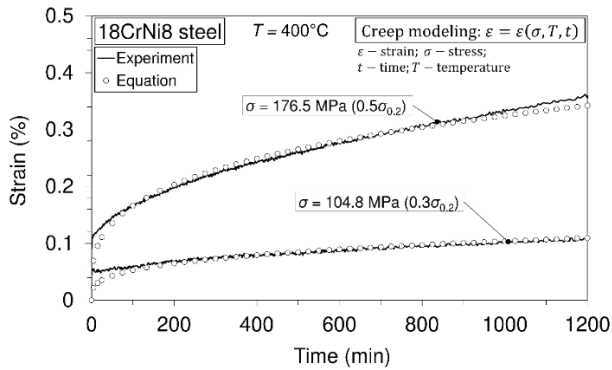


Fig. 9 Creep modeled curve at temperature of 500°C

$$\epsilon(t) = D^{-T} \sigma^p t^r \quad (1)$$

while the data related to creep modeling are given in Table 3.

The symbols used in Eq. (1) mean: ϵ -strain, T -temperature, σ -stress, and t -time, while D , p and r are the parameters, which are, to be determined. The modeled creep curves are shown in Figs. 8-9. The mark “equation” in the upper left corner of the images refers to the equation (1).

However, formula (1), as well as the mentioned rheological models, can be used in three different ways. One refers to the modeling of any creep curve separately at constant temperature (T_i) and at constant stress level (σ_i), i.e., ($\epsilon_t = \epsilon(t), \sigma_i = const, T_i = const$). The second refers to the entire stress range ($\sigma_1, \dots, \sigma_n$) within one constant temperature (T_i); i.e., ($\epsilon_t = \epsilon(\sigma, t), T_i = const$), and the third for the entire temperature range (T_1, \dots, T_n) and the full range of stresses ($\sigma_1, \dots, \sigma_n$) at any constant temperature (T_i) within the temperature range (T_1, \dots, T_n). The last mentioned model was applied to the temperature range 400°C – 500°C and for the stress levels shown in Table. 3. Although temperature range is quite narrow and stress levels within considered temperature range is also quite restricted, based on the presented modeled curves obtained using the formula, it is apparent that this kind of modeling is very successful. This is quite specific case since a small number of creep curves within a particular temperature is in the first or second stage of creep when formula (1) can be applied.

3.3 Charpy impact energy and fracture toughness assessment

As it is known, and already said, each engineering element is designed for a particular purpose. In this respect, for a particular element it is necessary to select the material resistant to high temperature, or high strength material, or material resistant to crack propagation, etc. For example, designers prescribe what should be the level of material toughness at a certain temperature, or what must be the value of the yield strength, or fracture toughness, etc. Namely, as previously said, many of failure modes can occur in engineering components. The task of the engineering failure analysis is to find an answer why and how some component has failed. Based on consideration of the basic design rules it is known that the yield strength ($\sigma_{0.2}$) is used as the most important factor against plastic deformation while fracture toughness (K_{Ic}) is used a factor

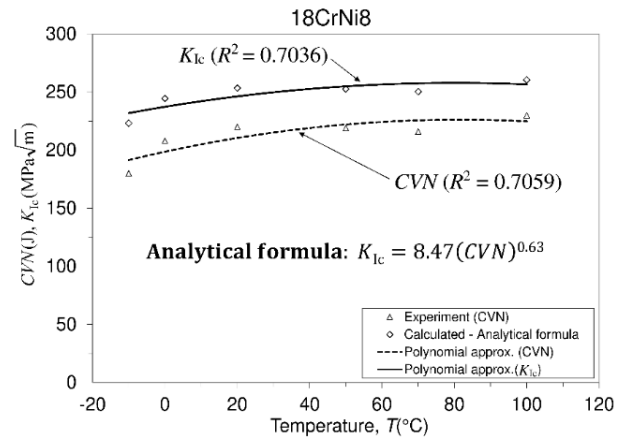
against fracture, i.e., crack propagation. As far as yield strength is concerned, the experimental results are shown earlier, Tab. 2. Fracture toughness, as a measure of material resistance against crack propagation usually is known as critical value of stress intensity factor (Suresh 2003), and can be experimentally determined. Dealing with the fracture toughness (K_{Ic}) means that there is no plastic area around the crack tip or it is very small. In terms of considering fatigue crack growth behavior, it is useful to gain insight into the paper written by Lu *et al.* (2019). Application of the Linear Elastic Fracture Mechanic (LEFM) has some limitation, i.e., experimentally obtained fracture parameter, called fracture toughness (K_{Ic}), is valid if some requirements are fulfilled. In general, it is valid as long as plasticity around the crack tip may be considered very small, Brnic (2018). In the cases when small-scale yielding is not valid, other elastic-plastic fracture parameters can be introduced, such as, for example J -contour integral. However, although fracture toughness can be experimentally determined, these results are only laboratory results and they are not determined based on the specimen extracted from the real structure.

From the other hand, it is not possible to manufacture a specimen from the finish product, and, specimen is quite large and its manufacture is complicated. To avoid the mentioned problems, and to avoid the problems with experimental testing of such a type that are very expensive and consume a lot of time, there are some much simpler experiments based on which good assessment of fracture toughness can be obtained. One such experiment is based on measuring the impact energy by Charpy impact machine. Based on the measured Charpy impact energy, an assessment of fracture toughness can be made. It should also be said that such tests also have some disadvantages. Namely, the dimensions and geometry of used Charpy V-notch specimen (CVN) comparing to the used specimen in fracture mechanics test can be quite different and specially different comparing with real structure conditions. Specimen used in Charpy test has a blunt notch while that in fracture mechanics test has sharp fatigue crack. Nevertheless, based on numerous tests during history, some correlations have been made between the results obtained by Charpy tests and those made according to other prescribed standard tests, Roberts and Newton (1981), and Shekhter *et al.* (2002). In chapter 2 is given data related to equipment, specimens and testing procedure in Charpy tests. Experimental results obtained using Charpy impact machine are shown in Fig. 10. Fracture toughness assessment based on impact energy was calculated by the Roberts-Newton formula (is valid regardless of temperature):

$$K_{Ic} = 8.47(CVN)^{0.63}; K_{Ic} (\text{MPa}\sqrt{\text{m}}), CVN (\text{J}) \quad (2)$$

3.4 Uniaxial fully reversed fatigue testing

The term “*fatigue*”, as a phenomenon, actually in descriptive clarification means “to tire”, Suresh (2003). Fatigue as one of possible failure modes is commonly associated with engineering and it is widely established in



$$K_{Ic}(T) = -3.18033 \cdot 10^{-3} T^2 + 5.11116 \cdot 10^{-1} T + 237.294$$

$$CVN(T) = -4.13833 \cdot 10^{-3} T^2 + 6.75536 \cdot 10^{-1} T + 198.617$$

Fig. 10 Charpy impact energy and fracture toughness (calculated values and polynomial approximations)

glossary as description for the damage / failure of material under cyclic load (stress). However, there are many different forms of fatigue failures. One of them, such as considered in this investigation, is so called *mechanical fatigue* caused by fluctuations in externally applied stresses. Further, acting of cyclic load in association with high temperature is known as *creep-fatigue*, then, *corrosion fatigue* can occur when repeated load is imposed in chemically aggressive environment, etc. Failure caused by repeated load can lead to the fracture at the stress that is much lower than fracture stress corresponding to a monotonic uniaxial strength. The level of the fracture stress at repeated load depends on several factors such as type of repeated load, stress ratio, material properties, etc. In any case, fatigue tests are very powerful tool showing the level of the fatigue strength corresponds to the number of the cycles to failure and in this sense test are useful tool for predicting the life of considered engineering element. Dependence of the number of the cycles to failure versus the applied level of the repeated stress usually is displayed in a coordinate system. On the ordinate is placed the level of the applied stress (maximum stress, mean stress, stress amplitude or similar), usually shown on a logarithmic or linear scale, while on the abscissa is placed the number of cycles to failure, usually shown on a logarithmic scale. Result of each fatigue test is plotted as one point in coordinate system.

3.4.1 Fatigue-life (S-N) diagram

Results of uniaxial fully reversed fatigue tests performed on unnotched specimens at room temperature and at stress ratio of $R = -1$, related to 18CrNi8 steel, are displayed in Fig.11. Diagram displayed is so –called Fatigue-life diagram. Test procedures that belong to the stress- life model were carried out under decreasing stress regime and in accordance with ISO standard (2012). As it is visible, maximum uniaxial stresses (σ_{max} , MPa) are placed on ordinate while the number of the cycles to failure (S) is placed on abscissa. Each test result is recorded as failed /broken (\blacklozenge) or unfailed /unbroken (\circ). Due to the

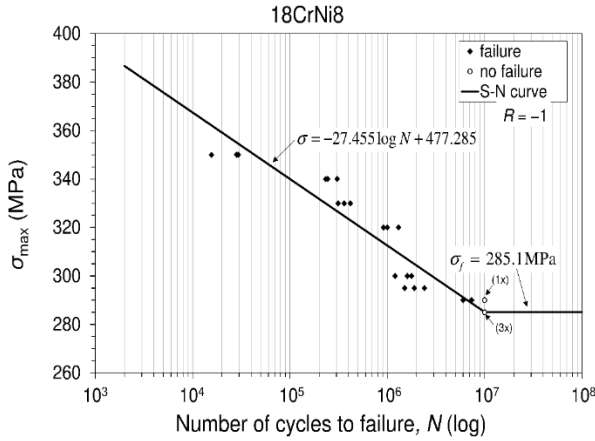


Fig. 11 Fatigue-life (S-N) diagram; stress ratio $R = -1$, 18CrNi8 steel

Table 4 Data for modified staircase method

Stress ratio $R = -1$, steel 18CrNi8							
Stress σ_i (max) (MPa)	Specimen						
	1	2	3	4	5	6	7
295			♦		♦		♦
290		♦		♦		○	
285	○						

possibility of the scatter of the results in the number of the cycles to failure, several tests were carried out for each level of applied maximum stress. After finishing the tests, as well as after determining the fatigue (endurance) limit using the modified staircase method, ISO standard (2012), a $S - N$ (fatigue-life, Wohler curve) diagram was obtained, as shown in Fig. 11.

Displayed $S - N$ diagram that represents fatigue behavior of the considered material consists of two areas. One area, represented by an inclined line, represents so called finite fatigue region (finite fatigue life), and another area, represented by a horizontal line, represents infinite fatigue region (infinite fatigue life). The horizontal line is essentially a fatigue limit and is obtained by a modified staircase method.

3.4.2 Fatigue (endurance) limit determination

The procedure for determination of the fatigue limit by modified staircase method proceeds as follows. Data related to the failed (♦) and unfailed (○) specimens that follow from fatigue tests are given in Tab. 4.

The analysis of data from Tab. 4 is presented in Tab. 5, while constants A, B, C and D are determined and shown in Tab. 6.

Fatigue limit (endurance limit, σ_f) calculation is proposed as follows (ISO standard 2012):

$$\sigma_{f(P,1-\alpha)} = \bar{\mu}_y - k_{(P,1-\alpha,dof)} \cdot \bar{\sigma}_y \quad (3)$$

In Eq. (3) are:

- $\bar{\mu}_y = \sigma_0 + d \left(\frac{A}{C} - \frac{1}{2} \right)$, the mean fatigue strength, (4)

Table 5 Data analysis for modified staircase method

Stress ratio $R = -1$, steel 18CrNi8; ($f = \text{failed}$)				
Stress σ_i (max) (MPa)	Stress level, i	f_i	if_i	$i^2 f_i$
295	2	3	6	12
290	1	2	2	2
285	0	0	0	0
$\sum f_i, if_i, i^2 f_i$		5	8	14

Table 6 A, B, C and D constants calculated (ISO 2012)

Stress ratio $R = -1$, steel 18CrNi8	
Formula	Material: 18CrNi8(1.5920)
$A = \sum i \cdot f_i$	8
$B = \sum i^2 \cdot f_i$	14
$C = \sum f_i$	5
$D = \frac{B \cdot C - A^2}{C^2}$	0.24

where σ_0 is the lowest stress level and “d” is the stress step (i.e., difference between the neighboring stress levels), \rightarrow Tab.5

- $k_{(P,1-\alpha,\nu)}$, the coefficient for the one sided tolerance limit for a normal distribution
- $\bar{\sigma}_y$, the estimated standard deviation of the fatigue strength that is calculated as

$$\bar{\sigma}_y = 1.62 \cdot d(D + 0.029). \quad (5)$$

Based on standard's recommendation, the value $\nu = n - 1 = 6$, where n is the number of items in a considered group. Further, for a desired probability of $P = 10\%$ and a confidence level $(1 - \alpha) = 90\%$, in accordance with the table B1, ISO standard (2012), it is: $k_{(P,1-\alpha,\nu)} = k_{(0.1;0.9;6)} = 2.333$. In accordance with Eq. (4), it is:

$$\text{for } R = -1 \rightarrow \bar{\mu}_y = \sigma_0 + d \left(\frac{A}{C} - \frac{1}{2} \right) = 285 + 5 \left(\frac{8}{5} - \frac{1}{2} \right) = 290.5 \text{ MPa,}$$

or, this can be obtained as (Tab. 4):

$$\text{for } R = -1 \rightarrow \bar{\mu}_y = (285 + 290 + 295 + 290 + 295 + 290 + 295) / 7 = 291.4 \text{ MPa,}$$

whose amount is similar to previously obtained ones.

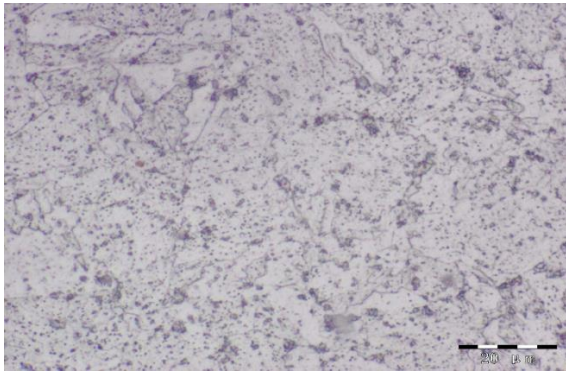
Now, in accordance with Eq. (5), it is:

$$\text{for } R = -1 \rightarrow \bar{\sigma}_y = 1.62 \cdot d(D + 0.029) = 1.62 \cdot 5 (0.24 + 0.029) = 2.1789 \text{ MPa.}$$

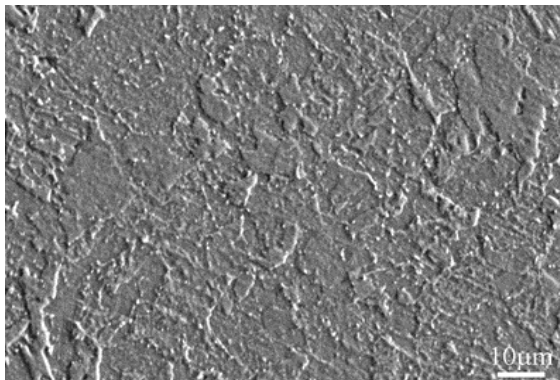
Finally, fatigue limit is (3):

$$\text{for } R = -1 \rightarrow \sigma_{f(0.1;0.9;6)} = \bar{\mu}_y - k_{(P,1-\alpha,\nu)} \cdot \bar{\sigma}_y = 290.5 - 2.333 \cdot 2.1789 = 285.1 \text{ MPa.}$$

Calculated value of the fatigue limit, based on the fatigue testing at stress ratio of $R = -1$, indicates that its value is 46% ($= 285.1/613$) compared with the ultimate monotonic stress.

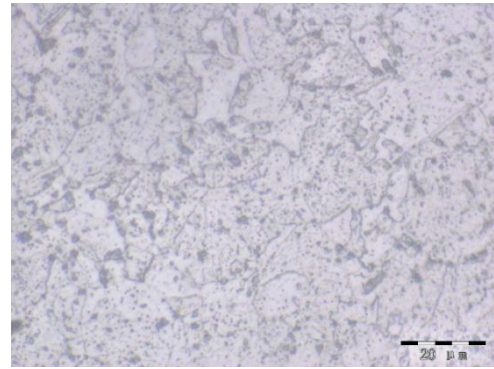


a) Optical micrograph

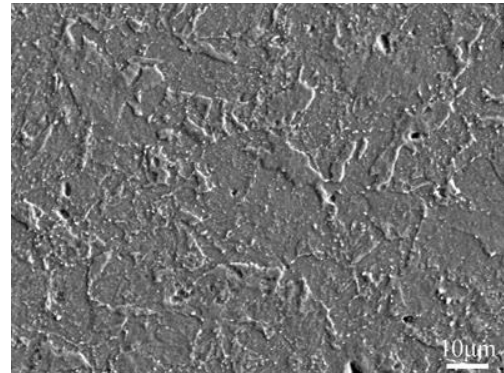


b) SEM micrograph

Fig.12 Optical and SEM micrographs: *As-received material* (specimen1), 18CrNi8 steel, 3% nitric acid, 97% alcohol, **cross-section**, 1000x

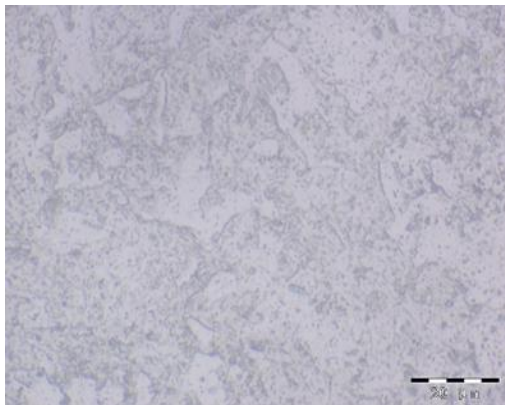


a) Optical micrograph

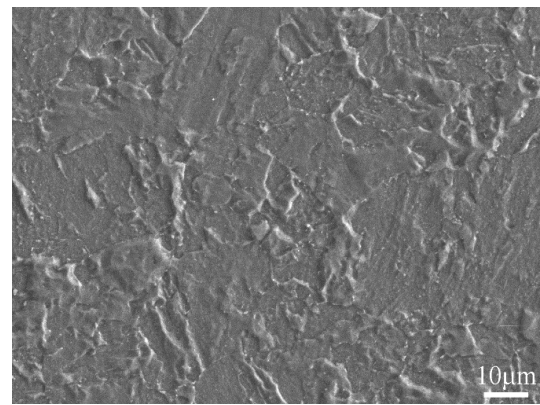


b) SEM micrograph

Fig.13 Optical and SEM micrographs: *Material previously subjected to creep* (specimen 2), at 500°C /82.8 MPa /1200 min, 18CrNi8 steel, 3% nitric acid, 97% alcohol, **cross-section**, 1000x



(a) Optical micrograph



(b) SEM micrograph

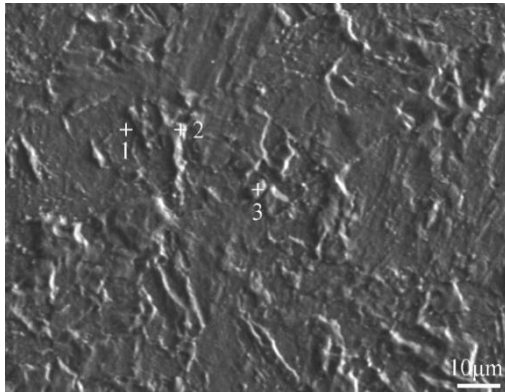
Fig.14 Optical and SEM micrographs: *Material fractured due to fatigue* (specimen 3), fractured at 305303 cycles, $\pm 340\text{MPa}$, 18CrNi8 steel, 3% nitric acid, 97% alcohol, **cross-section**, 1000x.

4. A short review of the microstructure analysis of material: As received, under creep and under fatigue

The main part of the content of the work is to analyze the mechanical behavior of materials in its different states. Accordingly, the microstructure analysis of the tested material in the mentioned states is done. In basic microstructure analysis of the as - received material

(specimen 1), material previously subjected to creep (specimen 2) and material subjected to fatigue (specimen 3), optical microscope (OM) as well as scanning electron microscope (SEM) were used. All of images made by optical or scanning electron microscope are presented in Figs. 12-17.

The images representing microstructure of the material in different states (specimen 1, specimen 2, specimen 3) were based on the cross-sections of the specimens. As for

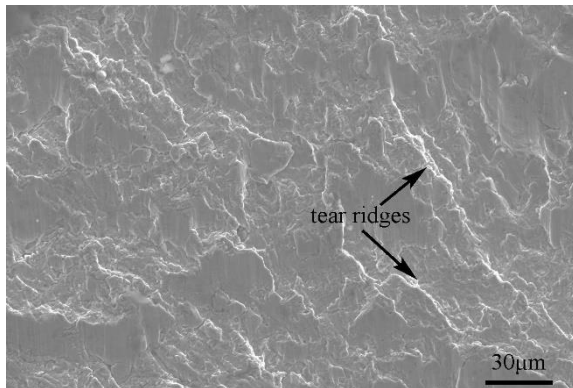


(a) SEM micrograph and corresponding positions 1, 2, 3

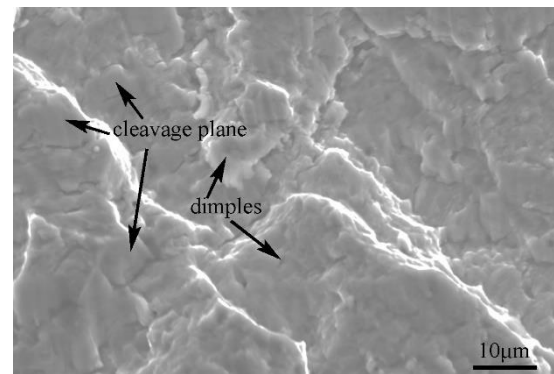
	Ni/at. %	Cr/at. %	Fe/at. %
position 1	1.481	2.1733	96.3457
position 2	1.5263	1.3747	97.0991
position 3	1.6284	2.1548	96.2168

(b) Compositions at corresponding positions

Fig. 15 SEM micrograph and the composition of the material at corresponding positions (1, 2, 3): **Material fractured due to fatigue** (specimen 3), fractured at 305303 cycles, $\pm 340\text{MPa}$, 18CrNi8 steel, 3% nitric acid, 97% alcohol, **cross-section**, 1000x.



(a) Tear ridges



(b) Cleavage planes

Fig. 16 SEM micrograph: **Fractured surface images of material fractured due to fatigue** (specimen 3), fractured at 305303 cycles, $\pm 340\text{MPa}$, 18CrNi8 steel,

specimen 1, representing the as-received material, whose microstructure is shown in Fig. 12a, obtained by optical microscopy, and in Fig. 12b obtained by SEM (scanning electron microscopy), it is found that microstructure composes of the majority of martensite and the minority of retained austenite. Regarding the specimen 2, representing the material previously subjected to creep, whose microstructure is presented in Fig. 13 also using optical microscopy as well as using SEM, it is also found that microstructure contains the majority of martensite and the minority of retained austenite, e.g., the same as for specimen 1 representing as-received material. Finally, regarding the microstructure of the specimen 3, shown in Fig. 14, representing the material fractured due to uniaxial fully reversed fatigue, it is found that the microstructure consists of the majority of martensite, minority of retained austenite and nano-sized precipitated phases. As shown in Fig. 15, representing SEM micrograph of the cross-section of specimen 3 (fractured specimen due to fatigue), and the composition in the corresponding positions, there are no significant differences in the composition of alloying elements among the three different scanning positions. As indicated in Fig. 16, numerous typical river-like patterns and

a large number of cleavage planes could be found. However, a small quantity of ductile fracture features such as tearing ridges and dimples could also be discovered. In this sense, it can be assessed that the fracture mode of the specimen 3 may be classified as the quasi-cleavage fracture. In accordance with XRD results, Fig. 17, it is visible that phases of specimen 1 confirm a small amount of carbides and a large amount of martensite which was actually Fe matrix solution containing a small quantity of Ni and Cr. However, austenite was not detected out in XRD patterns due to its low volume fraction. Moreover, there are no significant changes in phase constitution after creep and fatigue tests.

4. Conclusions

The main features of mechanical behavior of 18CrNi8 steel were determined in this research. Mechanical properties, creep resistance and fatigue limit as the results of research are of great importance in the design of elements made of this material. The ultimate tensile strength (σ_m) and yield strength ($\sigma_{0.2}$) vary in the range of $(\sigma_m/\sigma_{0.2}) \rightarrow [(613/458)\text{MPa}]_{20^\circ\text{C}}$ to $[(156/141)\text{MPa}]_{600^\circ\text{C}}$.

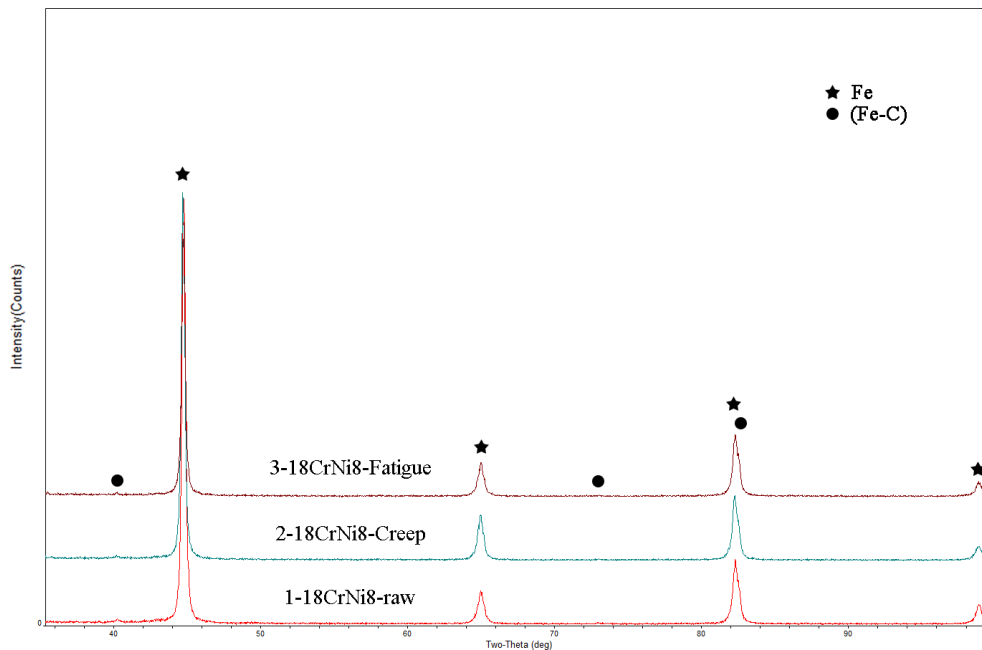


Fig. 17. XRD (X-ray diffraction) peaks / spectrum, for specimens 1-3 (1: as-received, 2: creep, 3: fatigue), 18CrNi8 steel

This steel is creep resistant to short-time creep at 400°C. At temperature of 500°C it is creep resistant if applied stress level does not exceed 30% of yield stress measured at this temperature. In addition, as the result of fully reversed fatigue tests performed at room temperature and using modified staircase method in fatigue limit calculation, fatigue limit is calculated in the amount of 285,1 MPa. This value is 46% comparing with the ultimate monotonic stress. Previously were mentioned possible engineering applications of this steel in the design of highly stressed shafts, gears and similar engineering elements of large cross-sections requiring high strength, good endurance limit and even high creep resistance in the cases of special environmental conditions such as any kind of hazard, fire or similar. All of mentioned applications may belong to mechanical engineering, aircraft industry, truck constructions, etc. Based on the conducted experimental studies, the obtained results relating to the mechanical properties of this material at different temperatures, its creep resistance and fatigue limit, show that this material can undoubtedly be used in constructions as mentioned above.

Acknowledgement

This work has been financially supported by the University of Rijeka within the projects: uniri-technic-18-42, "Investigation, analysis and modeling the behavior of structural elements stressed at room and high temperatures", uniri-technic-18-37, "Mechanical behavior of nanostructures" and uniri-technic-18-200, "Failure analysis of materials in marine environment". Authors are grateful to Professor Lin Geng from School of Material Science and Engineering, Harbin Institute of Technology, China, for analyzing the microstructure of the material.

References

- Ashby, M.F. (2011), *Materials Selection in Mechanical Design*, 4th Edition, Butterworth Heinemann, New York, NY, USA.
- ASTM (2016), "03.01:2016", *Mechanical Testing; Elevated and Low-Temperature Tests; Metallography*, ASTM Book of Standards Volume, ASTM, USA.
- Boresi, A.P., Schmidt, R.J. and Sidebottom, O.M. (1993), *Advanced Mechanics of Materials*, (5th Edition), John Wiley and Sons, New York, NY, USA.
- Bramfitt, B.L. (1997), "Effects of Composition, Processing and Structure on Properties of Irons and Steels", ASM Handbook, Volume 20, *Materials Selection and Design*, ASM International, USA.
- Brcic, J. (2018), *Analysis of Engineering Structures and Material Behavior*, (1st Edition), John Wiley & Sons, Chichester, United Kingdom.
- Brcic, J., Canadija, M., Turkalj, G., Krscanski, S., Lanc, D., Brcic, M. and Gao, Z. (2016), "Short-time creep, fatigue and mechanical properties of low alloy structural steel", *Steel Compos. Struct.*, **22**(4), 875-888. <https://doi.org/10.12989/scs.2016.22.4.875>.
- Brcic, J., Turkalj, G., Niu, J., Canadija, M. and Lanc, D. (2013), "Analysis of experimental data on the behavior of steel S275JR-Reliability of modern design", *Mater. Design*, **47**, 497-504. <https://doi.org/10.1016/j.matdes.2012.12.037>.
- Brooks, C.R. and Choudhury, A. (2002), *Failure Analysis of Engineering Materials*, McGraw Hill, New York, NY, USA.
- Collins, J.A. (1993), *Failure of Materials in Mechanical Design*, (2nd Edition), John Wiley & Sons, New York, NY, USA.
- Draper, N.R. and Smith, H. (1998), *Applied Regression Analysis*, Wiley-Interscience Publications, USA.
- Drozdov, A.D. (1996), *Finite Elasticity and Viscoelasticity*, World Scientific Publishing, New Jersey, NJ, USA.
- Findley, W.N., Lai, J.S. and Onaran, K. (1989), *Creep and Relaxation of Nonlinear Viscoelastic Materials*, Dover Publication, Inc., New York, NY, USA.
- Hosseini, S.R.E. (2012), "Simulation of case depth of cementation steels according to Fick's Laws", *J. Iron Steel Res.*, **19**(11), 71-

78. [https://doi.org/10.1016/S1006-706X\(13\)60023-0](https://doi.org/10.1016/S1006-706X(13)60023-0).
- Hosseini, S.R.E., Khosravi, H., Sohrabi, R., Hosseini, Z., Karimi, E. Z. and Makarem, M. (2013), "Correlation between hardenability curves and microstructure of a cementation steel carburized in the presence of Na₂CO₃ as an energizer material", *ISIJ International*, **53**(12), 2213-2217. <https://doi.org/10.2355/isijinternational.53.2213>.
- ISO (2012), "Metallic Materials-Fatigue Testing-Statistical Planning and Analysis of Data", 12107:2012, International Organization for Standardization, Geneva, Switzerland.
- Jana, S., Ramtekkar, T.R. and Ganguly, A. (2001), "Machinability characteristics of alloy and stainless steel bars", *Transactions of the Indian Institute of Metals*, **54** (1-2), 49-57.
- Kabira, M.J. and Bulpett, R. (2007), "A study of fatigue failure initiation in high cycle high-pressure automotive applications and conventional rotating bending fatigue testing", *J. Fatigue*, **29**(9-11), 1966-1970. <https://doi.org/10.1016/j.ijfatigue.2007.03.013>.
- Kong, Q.C., Li, Y., Liu, G.D., Li, C.J., Tong, H. and Gan, W.M. (2017), "Electrochemical machining for micro holes with high aspect ratio on metal alloys using three-electrode PPS in neutral salt solution", *J. Adv. Manufact. Technol.*, **93** (5-8), 1903-1913. <https://doi.org/10.1007/s00170-017-0645-y>.
- Lu, L., Li, J., Su, C. Yi, Sun, P. Y., Chang, L., Zhou, B. B., He, X., H., Zhou and Yu, C. (2019), "Research on fatigue crack growth behavior of commercial pure titanium base metal and weldment at different temperatures", *Theoretical Appl. Fracture Mech.*, **100**, 215-224. <https://doi.org/10.1016/j.tafmec.2019.01.017>.
- Raghavan, V. (2004), *Materials Science and Engineering*, Prentice-Hall of India, New Delhi, India.
- Roberts, R. and Newton, C. (1981), "Interpretive report on small-scale test correlation with K_{Ic} data", *Welding Research Council Bulletin*, **265**, 1-16.
- Shahraki, M., Sohrabi, M.R., Azizyan, G.R. and Narmashiri, K. (2018), "Experimental and numerical investigation of strengthened deficient steel SHS columns under axial compressive loads", *Struct. Eng. Mech.*, **67**(2), 207-217. <https://doi.org/10.12989/sem.2018.67.2.207>.
- Shekhter, A., Kim, S., Carr, D.G., Crocker, A.B.L. and Ringer, S.P. (2002), "Assessment of temper embrittlement in an ex-service 1Cr-1Mo-0.25V power generating rotor by Charpy V-notch testing; K_{Ic} fracture toughness and small punch test", *J. Pressure Vessels Piping*, **79**(8-10), 611-615. [https://doi.org/10.1016/S0308-0161\(02\)00087-X](https://doi.org/10.1016/S0308-0161(02)00087-X).
- Solecki, R.P. and Conant, R. (2003), *Advanced Mechanics of Materials*, Oxford University Press, New York, NY, USA.
- Stephens, R.I., Fatemi, A., Stephens, R.R. and Fuchs, H.O. (2001), *Metal Fatigue in Engineering*, (2nd Edition), John Wiley & Sons, New York, NY, USA.
- Suresh, S. (2003), *Fatigue of Materials*, (2nd Edition), Cambridge University Press, Cambridge, United Kingdom.
- Xu, X.L. and Yu, Z.W. (2015), "Cracking failure of locomotive diesel engine injector nozzles", *J. Failure Analysis Prevention*, **15**(4), 513-520. <https://doi.org/10.1007/s11668-015-9962-3>.
- Zhang, G., Kodur, V., Yao, W., Huang, Q. (2019), "Behavior of composite box bridge girders under localized fire exposure conditions", *Struct. Eng. Mech.*, **69**(2), 193-204. <https://doi.org/10.12989/sem.2019.69.2.193>.